# Modeling and Analysis : Energy Harvesting in the Internet of Things

Yu-Hsuan Chen
Department of Computer Science and Information Engineering
National Taiwan University, Taipei, Taiwan
r03922015@ntu.edu.tw

Bryan Ng
School of Engineering and Computer Science
Victoria University of Wellington, New Zealand
bryan.ng@ecs.vuw.ac.nz

Winston K.G. Seah
School of Engineering and Computer Science
Victoria University of Wellington, New Zealand
winston.seah@ecs.vuw.ac.nz

Ai-Chun Pang
Graduate Institute of Networking and Multimedia
National Taiwan University, Taipei, Taiwan
acpang@csie.ntu.edu.tw

## ABSTRACT

In the Internet of Things (IoT), the size constraint of those small and embedded devices limits the network lifetime because limited energy can be stored on these devices. In recent years, energy harvesting technology has attracted increasing attention, due to its ability to extend the network lifetime significantly. However, the performance of IoT devices powered by energy harvesting sources has not been fully analyzed and understood. In this paper, we model the energy harvesting process in IoT devices using slotted Carrier Sense Multiple Access with Collision Avoidance (CSMA /CA) mechanism of IEEE 802.15.4 standard, and analyze the performance in terms of delay and throughput. Our new model successfully integrates the energy harvesting process and binary backoff process through a unified Markov chain model. Finally, the new model is validated by simulation and the throughput errors between simulation and analytical model are no more than 6%. We demonstrate the application of the model with different energy harvesting rate corresponding to different sources such as solar and vibration energy harvesters.

## Keywords

Internet of Things, Energy Harvesting, IEEE 802.15.4 standard, CSMA/CA, Markov process

## 1. INTRODUCTION

The uses of Internet of Things(IoT) appears in a range of different domains [23] such as structural health monitoring, animal tracking and environmental surveillance. Despite the ubiquitous deployment of IoT devices, one prevailing problem with the network is the limited energy stored on each device. Replenishing the energy source by replacing batteries is a way to extend the network lifetime. However, in most applications it is difficult perhaps infeasible to replace the batteries because of the physical and environmental constraints. To deal with this problem, recent research efforts directed at designing energy efficient medium access control (MAC) protocols for IoT, and energy harvesting for IoT devices have emerged as a promising technique to prolong the network lifetime.

Powering IoT devices by energy harvesting technology is one half of the solution to the limited available energy while energy management is the other half. Since the energy harvesting rate is lower than the energy consumption rate [20], the sensing device stays awake for a short period of time after harvesting energy. Hence, the time spent harvesting energy must be taken into consideration when analyzing the performance of an energy harvesting IoT. Different MAC protocols for IoT with energy harvesting are analyzed through experiments, and the result shows that the energy harvesting process directly affects the performance of network throughput via the MAC protocols [5, 9].

The IEEE 802.15.4 MAC protocol is widely adopted in IoT for example, 6LoWPAN and ZigBee. It specifies the semantics for low-cost and low-power sensor networks operation. One of the access mechanisms specified by IEEE 802.15.4 standard is slotted Carrier Sense Multiple Access with Collision Avoidance (CSMA/CA) mechanism, and several simulation-based studies *e.g.,* [13, 15–17], analyze this protocol through Markov chain models. The Markov models for 802.15.4 that appear in [15–17] successfully predict the performance of the protocol in terms of delay, reliability, throughput and power consumption. However, these models assume that sensing devices have unlimited power, which limits the applicability of the model and simulation result in practical settings.

Some studies *e.g.,* [4, 8, 11, 21], have modelled the energy replenishment (recharging) process with varying degrees of success. A favoured approach for modelling the energy replenishment is the Markovian energy model which appears in [11] and [21]. The model in [11] assumes that the packet arrival and energy replenishment are both memoryless Poisson process, and the energy state transition follows the birth and death process. A further assumption is that packet



*MSWiM '16, November 13-17, 2016, Malta, Malta*



DOI: http://dx.doi.org/10.1145/2988287.2989144

transmissions are not interrupted by the energy replenishment, which is not valid in the real energy harvesting environment, but yields insights into how throughput is affected by energy harvesting process.

In [21], the energy model is modelled as a Bernoulli process and is unified with the slotted CSMA/CA mechanism of the IEEE 802.11 standard. In their model, the packet length and the backoff counter freezing time are not modelled, and the energy consumption during the channel sensing state is ignored, which does not reflect changes in residual energy correctly. In this paper, we model the slotted CSMA/CA mechanism of the IEEE 802.15.4 standard with the energy harvesting process through a unified Markov chain model. For simplicity, we assume that the network topology is a single hop network with a star topology. We derive the expressions for delay and throughput from the model, and validate the model through simulations. Through the proposed model, we characterize the effect of energy replenishment process on the performance of IEEE 802.15.4 MAC protocol, and show the effect of energy harvesting rate on the performance.

The contributions of this paper are: (i) a new model that integrates energy harvesting with slotted CSMA/CA mechanism of IEEE 802.15.4 standard within a unified Markov model, (ii) the energy harvesting process and the backoff process can take on different parameters and (iii) the energy consumption during binary backoff, clear channel assessment and packet transmission are necessarily distinct. Contributions (ii) and (iii) relaxes assumptions in existing models and reflects the real-world IoT devices behavior more closely.

The remainder of this paper is structured as follows. In Section II, we briefly describe the slotted CSMA/CA mechanism of the IEEE 802.15.4 standard, and explain how it interacts with the energy harvesting process. In Section III, we propose a Markov chain model of the slotted CSMA/CA mechanism integrated with the energy harvesting process. In Section IV, the model is validated by simulation and we compare the network performance with different energy harvesting rates. Section V concludes the paper.

## 2. OVERVIEW OF IEEE 802.15.4 SLOTTED CSMA/CA

In this section, we briefly explain the slotted CSMA/CA mechanism of the IEEE 802.15.4 standard [1], and highlight the interaction with an energy harvesting process. In the slotted CSMA/CA mechanism, there are three important variables [10] :

1. The *Number of Backoffs (NB)* is the number of times the algorithm has performed binary backoff before the packet transmission attempt. The value is initialized to 0 for a new transmission attempt.

2. The *Contention Window (CW)* is the number of backoff periods that the channel is required to be sensed idle before the transmission attempt. The value of $CW$ is initialized to $CW_0$. If the node operation is in the Japanese 950 MHz band, $CW_0$ shall be set to 1; otherwise, $CW_0$ shall be set to 2.

3. The *Backoff Exponent (BE)* controls the number of backoff periods that the algorithm needs to backoff before sensing the channel. The number of backoff periods is a random variable between [0, $2^{BE}$-1].

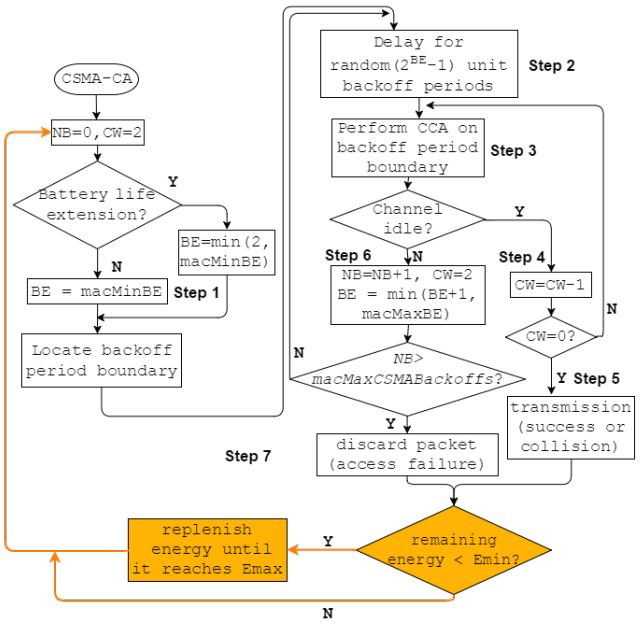


**Figure 1: Slotted CSMA/CA mechanism with energy harvesting**

Figure 1 is the flow chart of the slotted CSMA/CA mechanism with energy harvesting. First, the variables $NB$ and $CW$ are initialized to 0 and 2 respectively, while $BE$ is initialized to min (2, *macMinBE*) or *macMinBE* depending on the battery life extension(BLE). When BLE value is true, the MAC sublayer limits the random backoff exponent to ensure that the backoff duration, CCA and packet transmission is completed quickly (hence conserving energy). (**Step 1**). Next, the algorithm counts down a number of backoff periods which is randomly selected from [0, $2^{BE}$-1] (**Step 2**). After counting down to 0, the algorithm performs Clear Channel Assessment (CCA) to check if the channel is idle (**Step 3**). If the channel is idle, $CW$ is decreased by 1 (**Step 4**). If $CW$ is equal to 0, the packet can be transmitted (**Step 5**), or the CCA is repeated. If the channel is sensed busy, $NB$ is increased by 1, $CW$ is reinitialized and $BE$ is reinitialized to min($BE$+1, *macMaxBE*) (**Step 6**). If *macMaxCSMABackoffs* is reached, the packet is discarded (**Step 7**); otherwise, the backoff process restarts.

In this paper, we assume the MAC layer checks the remaining energy of the device after the packet transmission or access failure and this is shown in the orange shaded blocks in Fig. 1. If the energy is below a threshold denoted by $E_{\min}$, the energy harvesting process starts, and the energy is replenished before a new packet transmission attempt.

## 3. SYSTEM MODEL

In this section, we integrate an energy harvesting process to the IEEE 802.15.4 slotted CSMA/CA mechanism to characterize the performance of a network of IoT devices powered by energy harvesting. We focus on a single hop star network, in which every device transmits packets to the personal area network (PAN) coordinator and receives an acknowledgement (ACK). In the model, we assume that each device has a supercapacitor to store energy, and the maximum energy

**Table 1: Symbols used to describe the System Model**

| Symbol | Description |
|---|---|
| $m_0$ | *macMinBE* |
| $m$ | *macMAXCSMABackoffs* |
| $W_0$ | $2^{macMinBE}$ |
| $W_i$ | $2^i W_0$, for $1 \leq i \leq m$ |
| $E_{\max}$ | Maximum energy capacity of the supercapacitor |
| $E_{\min}$ | Minimum energy threshold, $L_t + (m+1) + 1$ |
| $L_0$ | The number of idle states |
| $L_t$ | Duration for packet transmission and receiving ACK |
| $P_c$ | Probability that collision occurs during packet transmission |
| $\alpha$ | Probability that the channel is busy in phase CCA1 |
| $\beta$ | Probability that the channel is busy in phase CCA2 |
| $q_0$ | Probability that the device keeps idle |

capacity of the supercapacitor is $E_{\max}$ unit.

During normal operation, defined as the MAC protocol in the following set of states: {idle, backoff, channel sensing, packet transmission}, energy is decreased. After the packet transmission process (success or collision) is finished, the device checks its remaining energy level. If the remaining energy is less than $E_{\min}$ units, the device halts operation and enters the energy harvesting process; otherwise, the device waits for a new packet arrival.

## 3.1 Energy harvesting process

Energy harvesting is the process by which ambient energy is captured and stored in the supercapacitor. We assume that the energy harvesting process follows the Poisson process to reflect the deployments of IoT in several sensor network scenarios such as structural health monitoring environments [6], bridge monitoring [3] and harvesting solar energy in situations whereby the solar irradiance is variable due to the passing of clouds [2]. The energy harvesting process stops when the energy level in the supercapacitor reaches $E_{\max}$ and the CSMA/CA mechanism restarts operation.

## 3.2 State space of the Markov model

The Markov chain model for the IEEE 802.15.4 slotted CSMA/CA mechanism with energy harvesting is shown in Fig. 2. The state space is categorized into four sets of states and each set is characterized with different indices. Let $e(t)$, $f(t)$, $h(t)$, $s(t)$ and $k(t)$ be stochastic processes representing the the backoff stage number, the state of the backoff counter, the residual energy level of a device, the energy harvested and the number of packets awaiting transmission at time $t$ respectively. The tuple $\{\delta(t), e(t), f(t), h(t)\}$ form the set of **transmission states** whereby $\delta(t)$ is the indicator process of a successful transmission or otherwise defined in Eq.(1). This set of states are grouped and labelled as "Tx #0" and "Tx #$m$" in Fig.2(a).

$$\delta(t) = \begin{cases} -1 & \text{if transmission successful at time } t \\ -2 & \text{if transmission unsuccessfull at time } t \end{cases} \quad (1)$$

Transmission states $\{-1, i, j, s\}$ and $\{-2, i, j, s\}$ represent the successful and collided packet transmissions respectively with the indices bounded by $i \in [0, m]$, $j \in [0, L_t - 1]$ and $s \in [E_{\max} - 2 - m - L_t, E_{\max} - m - 3]$.

The backoff process is characterised by stochastic processes $e(t), f(t)$ and $h(t)$ and the tuple $\{e(t), f(t), h(t)\}$ denotes the set of **backoff states** and the set of **CCA states** (these sets are labelled as "Backoff" and "Idle" in Fig. 2(a). Backoff states $\{i, w, s\}$ are bounded by $i \in [0, m], w \in [1, W_i - 1]$, in which $i$ is the backoff stage, and $w$ is the backoff counter. The first phase (CCA1) and the second phase (CCA2) of the CCA are denoted by states $\{i, 0, s\}$ and $\{i, -1, s\}, i \in [0, m]$ respectively.

The behaviour of an idle device waiting for a new packet arrival is modelled by $k(t)$ and $s(t)$, therefore the tuple $\{k(t), s(t)\}$ denotes the set of **idle states** with the tuple defined in the range of $\{c, s\}$, $c \in [0, L_0 - 1]$, $s \in [0, E_{\max} - 1]$. Note that the degree of traffic saturation is regulated through the parameter $L_0$. Finally, the energy harvesting is governed by a single process $s(t)$ with $s \in [0, E_{\max} - 1]$ and it forms a sub-chain shown in Fig.2(c).

The variable $L_t$ denotes the number of backoff periods for packet transmission and receiving ACK and it is expressed as $L_t = L + t_{\text{ack}} + L_{\text{ack}}$, where $L$ is the number of backoff periods for packet transmission, $t_{\text{ack}}$ is the idle period between the packet transmission and receiving ACK, and $L_{\text{ack}}$ is the number of backoff periods for receiving ACK. Based on the 802.15.4 standard specifications [1] we set $t_{\text{ack}} = 1$ backoff period and $L_{\text{ack}} = 2$ backoff periods. Throughout this paper, we assume that the duration for successful packet transmission and the duration for collided packet transmission are identical.

Recall that the states $s \in [0, E_{\max} - 1]$ are energy harvesting states with $s$ representing the residual energy level of the device, and the energy harvesting is governed by a Poisson process with rate $\lambda$. The value of $\lambda$ dictates the energy units harvested in a backoff period. According to the energy consumption rates in different states, we assume that there is no energy consumption in backoff states [17]. In our model, idle states collectively consume one unit of energy, thus CCA1 and CCA2 together consume one unit energy, and each of the transmission state consumes one unit of energy. The value of $E_{\min}$ is the sum of the energy consumed during packet transmission, the total number of backoff stages, and the energy consumed in idle states, thus:

$$E_{\min} = L_t + (m+1) + 1.$$

In Fig. 2(c), the constant $e$ is equal to $E_{\min} - 1$. Table 1 lists the symbols and the meanings in the context of the Markov model.

## 3.3 State transitions

Our model in Fig. 2 is composed of layers, and these layers are linked to energy harvesting states. Each layer has the same structure in terms of states and transitions. When a device terminates packet transmission and the remaining energy level $s$ is greater than $E_{\min}$, the device transits to the idle state in another layer with probability $q_0$, or transits to the backoff state with probability $1 - q_0$. But if $s$ is less than $E_{\min}$ unit, the device transits to the energy harvesting state. For example, if the packet transmission is done in the state $(-1, 0, L_t - 1, E_{\max} - 2 - L_t)$ and $(E_{\max} - 2 - L_t)$ is greater than $E_{\min}$, the state of the device transits to the idle state $(0, (E_{\max} - 2 - L_t) - 1)$ with probability $q_0$.

The index of a layer models the remaining energy level of the device when in idle states and this index is an integer

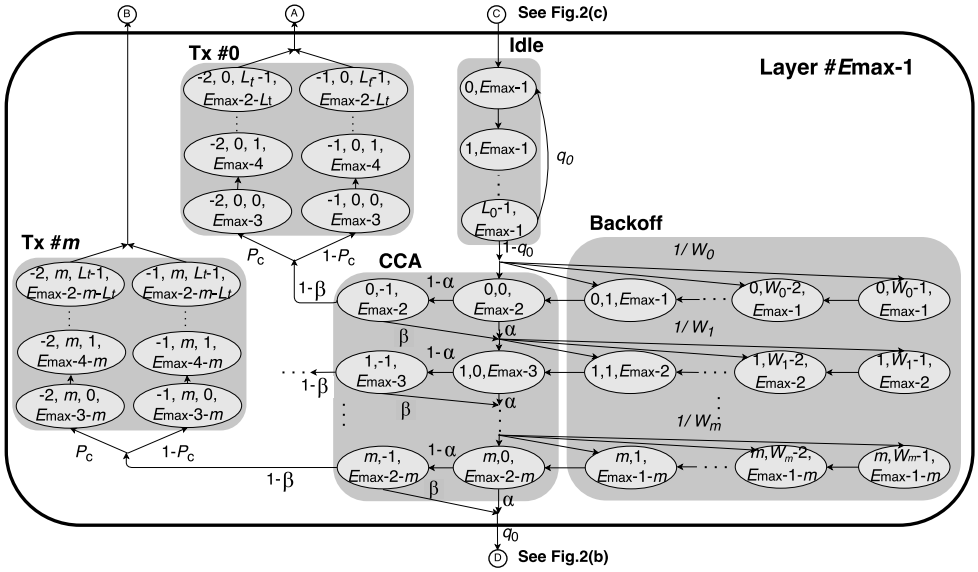


(a) Transitions and states of the Markov chain model for CSMA/CA depicted as a single layer.

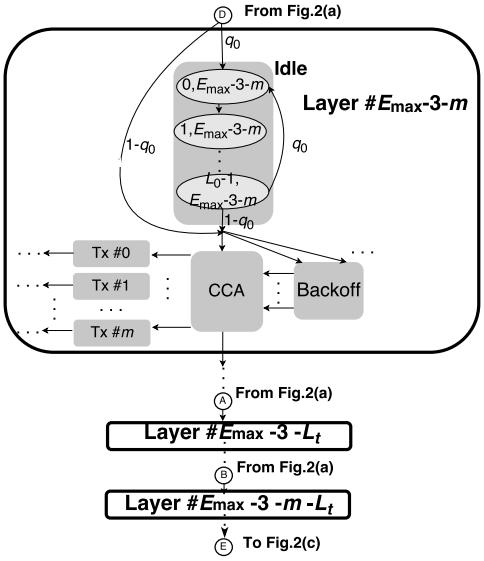


(b) Transitions between adjacent CSMA/CA backoff layers. This figure is connected to Fig. 2(a).

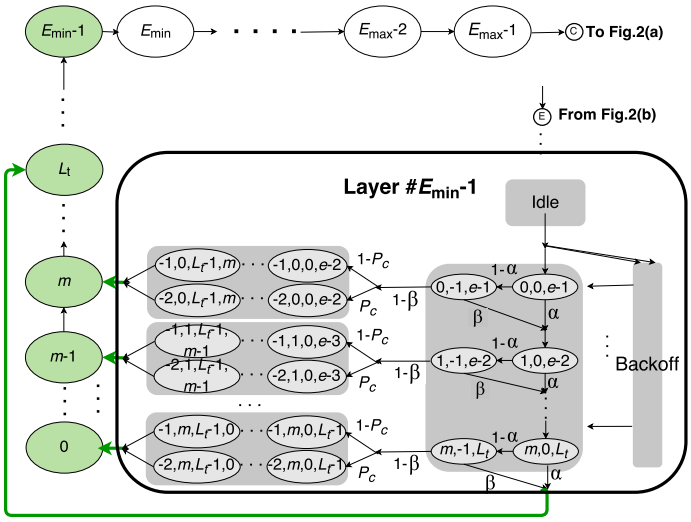


(c) Transitions and states of the energy harvesting sub-chain.

**Figure 2: Markov model**

defined over the range of $E_{\min}-1$ to $E_{\max}-1$. In energy harvesting states, the permissible state transitions are shaded (green in Fig. 2(c)) and the sojourn time of energy harvesting states follows an exponential distribution.

Using simplified notation $\Pr\{\mathcal{E}\}$ where $\mathcal{E}$ denotes a transition event of the MAC, the non-null state transition probabilities of the Markov chain are:

$$\begin{aligned}
&\Pr\{\text{harvesting one unit of energy}\}\\
&\quad = P(s+1|s) = e^{\lambda}\lambda, \qquad \text{for } 0 \le s < E_{\max}-1, \qquad (2)\\
&\Pr\{\text{transit to the first backoff stage from an idle state}\}\\
&\quad = P(0,w,s|L_0,s)\\
&\quad = P(0,0,s-1|L_0,s)\\
&\quad = \frac{1-q_0}{W_0}, \qquad \text{for } 1 \le w < W_0, \qquad (3)\\
&\Pr\{\text{the decrement of the backoff counter}\}\\
&\quad = P(i,w-1,s|i,w,s)\\
&\quad = P(i,0,s-1|i,1,s)\\
&\quad = 1, \qquad \text{for } 0 \le i \le m \text{ and } 1 < w < W_0, \qquad (4)\\
&\Pr\{\text{new backoff after channel sensed busy during CCA1 or CCA2 }\}\\
&\quad = P(i,w,s|i-1,0,s)\\
&\quad = P(i,0,s-1|i-1,0,s)\\
&\quad = \frac{\alpha+(1-\alpha)\beta}{W_i}, \qquad \text{for } 1 \le i \le m \text{ and } 1 \le w < W_i, \qquad (5)\\
&\Pr\{\text{channel is idle during CCA1 and CCA2,}\\
&\qquad \text{upon a successful packet transmission}\}\\
&\quad = P(-1,i,0,s-1|i,0,s)\\
&\quad = (1-\alpha)(1-\beta)(1-P_c), \qquad (6)\\
&\Pr\{\text{channel is idle during CCA1 and CCA2,}\\
&\qquad \text{after a collision}\}\\
&\quad = P(-2,i,0,s-1|i,0,s)\\
&\quad = (1-\alpha)(1-\beta)P_c. \qquad (7)
\end{aligned}$$

The probability that the device is in the wait state (awaiting packet arrivals) or is charged after the transmission is denoted by Eq. (8) and Eq. (9) respectively. Therefore, the non-null transition probabilities are:

$$\begin{aligned}
&\Pr\{\text{waiting state after a packet transmission}\}\\
&\quad = P(0,s-1|-1,i,L_t-1,s)\\
&\quad = P(0,s-1|-2,i,L_t-1,s) = \begin{cases} q_0, & \text{if } s \ge E_{\min}\\ 0, & \text{if } s < E_{\min}\end{cases}, \qquad (8)\\
&\Pr\{\text{energy harvesting after the packet transmission}\}\\
&\quad = P(s|-1,i,L_t-1,s)\\
&\quad = P(s|-2,i,L_t-1,s) = \begin{cases} 0, & \text{if } s \ge E_{\min}\\ 1, & \text{if } s < E_{\min}\end{cases}. \qquad (9)
\end{aligned}$$

If the remaining energy level is below $E_{\min}$, the device halts normal operation and the energy harvesting process starts. Subsequently, the probability that the device is in a wait state (awaiting packet arrival) or is charged after the access failure is given by Eq. (10) and Eq. (11). The device waits for a new packet arrival only if the remaining energy level is above $E_{\min}$. Thus, the non-null transition probabilities are:

$$\begin{aligned}
&\Pr\{\text{waiting state after an access failure}\}\\
&\quad = P(0,s-1|m,0,s)\\
&\quad = \begin{cases} q_0 \times (\alpha+(1-\alpha)\beta), & \text{if } s \ge E_{\min}\\ 0, & \text{if } s < E_{\min}\end{cases}, \qquad (10)\\
&\Pr\{\text{energy harvesting after the access failure}\}\\
&\quad = P(s|m,0,s) = \begin{cases} 0, & \text{if } s \ge E_{\min}\\ \alpha+(1-\alpha)\beta, & \text{if } s < E_{\min}\end{cases}. \qquad (11)
\end{aligned}$$

## 3.4 Stationary distribution

The stationary distribution of the embedded Markov chain of Fig. 2 is a vector $\boldsymbol{\pi}$. For ease of presentation, we decompose the vector into four different states:

- **idle states**, the stationary probability is
$$\pi_{c,s}, c \in (0, L_0-1), s \in (E_{\min}-1, E_{\max}-1),$$
- **backoff / CCA states**, the stationary probability is
$$\pi_{i,w,s}, i \in (0,m), w \in (-1, W_i-1),$$
- **packet transmission states**, the stationary probability is
$$\pi_{-1,i,j,s} \text{ and } \pi_{-2,i,j,s}, i \in (0,m), j \in (0, L_t-1),$$
- **energy harvesting states**, the stationary probability is
$$\pi_s, s \in (0, E_{\max}-1),$$

such that

$$\boldsymbol{\pi} = (\pi_{c,s} \cup \pi_{i,w,s} \cup \pi_{-1,i,j,s} \cup \pi_{-2,i,j,s} \cup \pi_s).$$

Using this notation, the transition probabilities that appear earlier in Eq. (3) and Eq. (4) are simplified to:

$$\pi_{i,w,s+1} = \frac{W_i - w}{W_i}\pi_{i,0,s}, \qquad (12)$$

where $w$ is from 1 to $W_i - 1$. Similarly, the transition probabilities in Eq. (5) are expressed as

$$\pi_{i,0,s-i} = (\alpha+(1-\alpha)\beta)^i \pi_{0,0,s}. \qquad (13)$$

Summing the state probabilities for a layer indexed by $s$ (i.e. Eq. (3) - (7), Eq. (12) and Eq. (13)), we obtain the probability the Markov chain is in layer $s$:

$$\begin{aligned}
&L_0 \times \pi_{0,s} + \frac{\pi_{0,0,s-1}}{2}\left(\frac{1-(2x)^{m+1}}{1-2x}W_0 + \frac{1-x^{m+1}}{1-x}\right)\\
&\qquad + (1-\alpha)\frac{1-x^{m+1}}{1-x}\pi_{0,0,s-1} + L_t(1-x^{m+1})\pi_{0,0,s-1}\\
&= \pi_{0,s} \times L_0 + \pi_{0,0,s-1} \times\\
&\quad \left\{\frac{1-(2x)^{m+1}}{2(1-2x)}W_0 + \frac{1-x^{m+1}}{1-x}\left[\frac{3}{2} - \alpha + (1-x)L_t\right]\right\}, \qquad (14)
\end{aligned}$$

where $x = \alpha + (1-\alpha)\beta$.

From Eq. (14) we expand the expressions for $\pi_{0,s}$ and $\pi_{0,0,s-1}$ and this yields:

$$\pi_{0,s} = \begin{cases} \frac{\pi_{E_{\max}-1}}{1-q_0}, & \text{if } s = E_{\max}-1 \\ \frac{q_0(Q_a(s)+Q_b(s))}{1-q_0}, & \text{otherwise} \end{cases}, \quad (15)$$

and $\pi_{0,0,s-1}$ is given by:

$$\pi_{0,0,s-1} = \begin{cases} (1-q_0)\pi_{0,s}, & \text{if } s = E_{\max}-1 \\ (1-q_0)(Q_a(s)+Q_b(s)+\pi_{0,s}), & \text{otherwise} \end{cases}, \quad (16)$$

where $Q_a(s)$ is the state transition probability to layer $s$ due to the packet transmission and $Q_b(s)$ is the state transition probability to $s$ conditioned on access failure. Using Eq. (15) and Eq. (16), we establish the relationship between $\pi_{0,s}$ and $\pi_{0,0,s-1}$ which expresses the probability the Markov chain is in state $s$ (Eq. (14)) as a function of $\pi_{0,s}$.

The derivation of $Q_a(s)$ is as follows: we introduce the auxiliary variable $r = (s+1) + L_t$, to denote the remaining energy level of the device during its successful CCA1 and CCA2. For $r+1 > E_{\max}-1$, the corresponding $Q_a(s)$ is 0, while for $r+1 \le E_{\max}-1$, we obtain $Q_a(s)$ as:

$$\begin{aligned} Q_a(s) &= \sum\nolimits_{i=(r+1)+0}^{n} (1-\alpha)(1-\beta)\pi_{i-(r+1),0,r} \\ &= \sum\nolimits_{i=(r+1)+0}^{n} (1-\alpha)(1-\beta)x^{i-(r+1)}\pi_{0,0,i-1}, \end{aligned}$$

where $(r+1)$ and $n = \min(E_{\max}-1,\ (r+1)+m)$ are the respective minimum and maximum index of layers that the state transition from these layers to state $(0,s)$ after the packet transmission exists. This relationship is direct from Eq. (6) and Eq. (7). Moreover, from Eq. (10), the expression for $Q_b(s)$ is readily obtained as:

$$Q_b(s) = \begin{cases} 0, & \text{if } d > E_{\max}-1 \\ x \times \pi_{m,0,s+1}, & \text{if } d \le E_{\max}-1 \end{cases}, \quad (17)$$

where $d = (s+1)+m+1$, which is the index of the layer and the state transition from the layer to state $(0,s)$ after an access failure. When $d \le E_{\max}-1$, the probability the Markov chain transits to state $s$ can be rewritten as follows:

$$Q_b(s) = x \times \pi_{m,0,s+1} = x^{m+1}\pi_{0,0,d-1}.$$

Now, we will derive the stationary distribution expressions for the energy harvesting states $\pi_s, s \in (0, E_{\max}-1)$. Starting from the expressions in Eq. (2), Eq. (9) and Eq. (11), we have:

$$\pi_s = \begin{cases} R_a(s)+R_b(s), & \text{if } s = 0 \\ R_a(s)+R_b(s)+\pi_{s-1}, & \text{if } 0 < s \le E_{\min}-1 \\ \pi_{E_{\min}-1}, & \text{if } E_{\min}-1 < s \end{cases} \quad (18)$$

where $R_a(s)$ is the probability that the device starts energy harvesting process with remaining energy level $s$ after the packet transmission, and $R_b(s)$ is the probability that the device starts energy harvesting process with remaining energy level $s$ after the access failure.

The derivation of $R_a(s)$ is similar to that of $Q_a(s)$. Denote the remaining energy level of the device during its successful CCA1 and CCA2 by $u$ such that $u = s + L_t$. When $u+1 > E_{\max}-1$, the value of $R_a(s)$ is 0. When $u+1 \le E_{\max}-1$, the expression of $R_a(s)$ is

$$\begin{aligned} R_a(s) &= \sum\nolimits_{i=v}^{k} (1-\alpha)(1-\beta)\pi_{i-(u+1),0,u} \\ &= \sum\nolimits_{i=v}^{k} (1-\alpha)(1-\beta)x^{i-(u+1)}\pi_{0,0,i-1}, \end{aligned} \quad (19)$$

where $v = \max(u+1, E_{\min}-1)$ and $k = \min((u+1)+m, E_{\max}-1)$ are the minimum and maximum index of those layers that can transit to state $(s)$ after the access failure, respectively. The expression of $R_b$(s) is

$$R_b(s) = \begin{cases} 0, & \text{if } s+m+1 < E_{\min}-1 \\ 0, & \text{if } s+m+1 > E_{\max}-1 \\ x \times \pi_{m,0,s}, & \text{if } E_{\max}-1 \ge s+m+1 \ge E_{\min}-1 \end{cases}. \quad (20)$$

When $s+m+1 \ge E_{\min}-1$, we can rewrite $R_b(s)$ as

$$x \times \pi_{m,0,s} = x^{m+1}\pi_{0,0,s+m}$$

The probability of each state in Eq. (14) - (20) can be rewritten as a function of $\pi_{0,0,s-1}$, $s \in (E_{\min}-1, E_{\max}-1)$. Given that we have derived the relations of $\pi_{0,s}$ and $\pi_{0,0,s-1}$, the sum of the stationary probability of Markov chain can further be expressed by $\pi_{0,E_{\max}-1}$.

We now derive the remaining unknowns $\alpha$, $\beta$ and $P_c$ by considering the sojourn time of the states. Let $\boldsymbol{P}$ be the limiting probability of the Markov chain in Fig. 2. For CCA1 states, the limiting probability $P_{i,0,s}$ and its relationship with $\pi_{i,0,s}$ is given by:

$$P_{i,0,s} = \lim_{t\to\infty} P_{i,0,s}(t) = \frac{\pi_{i,0,s}E(T_{i,0,s})}{\sum_{k\in S}\pi_k E(T_k)},$$

where $T_k$ is the sojourn time of state $k$, and $S$ presents a set of discrete states of the Markov chain. Because the sojourn time of each state in each layer is normalized to a unit backoff period, and the sojourn time of energy harvesting states depends only on the harvesting rate $\lambda$, the limiting probability of CCA1 states is readily expressed as a function of $\pi_{0,E_{\max}-1}$.

Next, we introduce a probability $\tau$ that the device performs its CCA1 in a random backoff period, which is equal to the sum of the limiting probability of CCA1 states. Similar to [16], the value of $\tau$ is given by

$$\tau = \sum_{s=E_{\min}-2}^{E_{\max}-2} \frac{1-x^{m+1}}{1-x} P_{0,0,s}. \quad (21)$$

Now, we can derive the probabilities $\alpha$, $\beta$ and $P_c$. The conditional collision probability $P_c$ is the probability that the collision occurs during packet transmission. In the slotted CSMA/CA mechanism, a collision occurs only if at least one of the remaining $N-1$ devices start packet transmission in a same backoff period. Hence, $P_c$ is

$$P_c = 1-(1-\tau)^{N-1}, \quad (22)$$

where $N$ is the number of nodes.

The probabilities $\alpha$ and $\beta$ are the probabilities that the channel is sensed busy during CCA1 and CCA2:

$$\alpha = \alpha_1 + \alpha_2, \quad (23)$$

where $\alpha_1$ is the probability that the channel is sensed busy during CCA1 due to the packet transmission (the proof of (23) appears in [17] and [16].) Since the probability that a

device starts to transmit a packet is $\tau(1-\alpha)(1-\beta)$, and $1-(1-\tau)^{N-1}$ is the probability that at least one of the $N-1$ remaining devices stay in CCA1 states, $\alpha_1$ is

$$\alpha_1 = L(1-(1-\tau)^{N-1})(1-\alpha)(1-\beta)$$

and $\alpha_2$ is the probability that the channel is sensed busy during CCA1 due to ACK transmission, which is expressed as:

$$\begin{aligned}\alpha_2 &= L_{ack}\frac{N\tau(1-\tau)^{N-1}(1-\alpha)(1-\beta)}{(1-(1-\tau)^N)(1-\alpha)(1-\beta)} \\ &\quad \times (1-(1-\tau)^{N-1})(1-\alpha)(1-\beta) \\ &= L_{ack}\frac{N\tau(1-\tau)^{N-1}}{1-(1-\tau)^N}(1-(1-\tau)^{N-1})(1-\alpha)(1-\beta),\end{aligned}$$

where $(1-(1-\tau)^N)(1-\alpha)(1-\beta)$ is the probability that at least one device can transmit a packet, and $N\tau(1-\tau)^{N-1}(1-\alpha)(1-\beta)$ is the probability that only one device is transmitting the packet. The probability that the channel is sensed busy (denoted by $\beta$):

$$\beta = \frac{1-(1-\tau)^{N-1}+N\tau(1-\tau)^{N-1}}{2-(1-\tau)^N+N\tau(1-\tau)^{N-1}}. \quad (24)$$

Further details about deriving the probabilities $\alpha$, $\beta$ and $P_c$ appear in [17]. With the complete characterization of these transition probabilities, the model is solved numerically.

# 4. MODEL VALIDATION

In this section, we validate the proposed model by simulation, and analyze the performance in terms of delay, throughput and reliability. The simulation is developed in Matlab.

## 4.1 Simulation Setup

The algorithm follows the pseudo code proposed in [17] and we extend it to accommodate acknowledgements and the unsaturated traffic conditions. Because the device only changes state at the backoff period boundaries, we normalize the simulation step to one backoff period. The total simulation time is $10^8$ backoff periods. The simulation is performed 10 times with different random seeds, and it shows that the percentage differences of each result value and the average value are all less than 1%.

## 4.2 Expression of Throughput and Delay

The average throughput from the simulation is simply:

$$\text{Throughput(sim)} = \frac{n_s \times L}{T_{\text{simulation}}}$$

where $n_s$ denotes the number of successfully transmitted packets, and $T_{\text{simulation}}$ refers to the total simulation time. The unit of the packet length $L$ and the unit of simulation time are both a backoff period. Similarly to [17], we derive the average throughput from our analytical model in Section III by the following expression:

$$\text{Throughput(ana)} = LN\tau(1-\tau)^{N-1}(1-\alpha)(1-\beta)$$

Next, we derive the average delay. We define the average delay of a packet as the time from the first attempt of backoff, until the time when the ACK is received. Consistent with the analytical model, we do not consider the delay of discarded packets due to the collision or access failure. The expression of the average delay is as follows:

$$\text{Delay(sim)} = \frac{T_{\text{delay}}}{n_s} \times T$$

where $T_{\text{delay}}$ denotes the sum of packets' delay while $T$ is the length of the backoff period. According to IEEE 802.15.4 standard [1], a backoff period is 20 symbols long (*aUnitBackoffPeriod*), and 1 symbol is 4 bits. For a typical bit rate of 250kbps, $T$ is $\frac{80\text{bits}}{250\text{kbps}} = 0.32\text{ms}$.

The derivation of the average delay from the analytical model is similar to that in [16]. However, in our model, we assume that the packet is dropped if the collision or access failure occurs, so $macMaxFrameRetries = 0$.

**Table 2: energy harvesting rate with 10cm$^2$ or 10cm$^3$ harvesting material**

| Material | Power Density ($\mu$W/cm$^2$) | Energy Harvesting Rate (mW) | Energy Harvesting Rate$^\dagger$ |
|---|---|---|---|
| Electromagnetic [19] | 433$^{**}$ | 4.33 | 0.144 |
| Piezoelectric [7] | 106.9$^{**}$ | 1.069 | 0.0356 |
| Electrostatic (Triboelectric) [18] | 0.648 | 0.0064 | 0.0002 |
| Thermoelectric [12] | 60 | 0.6 | 0.02 |
| Solar - direct sunlight [14] | 16800 | 168 | 5.6 |

$^\dagger$ the energy units harvested in a backoff period
$^{**}$ unit is $\mu$W/cm$^3$

## 4.3 Model Validation and Performance Analysis

The energy harvesting rates from different energy harvesting technologies with dimension 10cm$^2$ or 10cm$^3$ is listed in Table 2. In [19], they harvested energy through an electromagnetic transducer constructed with two permanent magnets and a 11cm$^3$ coil. Output power of 4.33mW is achieved with a 90$\Omega$ load resistor connected to the transducer. In [7], the energy is harvested using piezoelectric bimorph/magnet compsites and an AC power line. When the power is switched on, the AC magnetic field interacts with the magnetization of the magnet inciting the piezoelectric cantilever. In [18], they implement the electrodes, diode ladder circuit and a energy harvesting circuit on skirt paddles. Due to the triboelectric effect, these paddles generate electrostatic energy when brushed rapidly against each other.

In [12], they wear the 9cm$^2$ thermoelectric energy harvester on the wrist. Using the temperature difference between the skin and ambient temperature, the thermoelectric energy is generated. The maximum generated power is about 60$\mu$W/cm$^2$ indoors and about 600$\mu$W/cm$^2$ at a temperature of 0$^\circ$C. In [14], the National Institute of Water and Atmospheric Research(NIWA) conducts the SolarView calculation for a year in Kelburn, Wellington. The average Solar Energy reachers 168mW.

In this paper, we assume that the energy consumption rate for packet transmission is 30mW [16], and the actual length of a backoff period is 0.32ms. Using this relationship, the energy harvesting rate from mW is easily converted to the

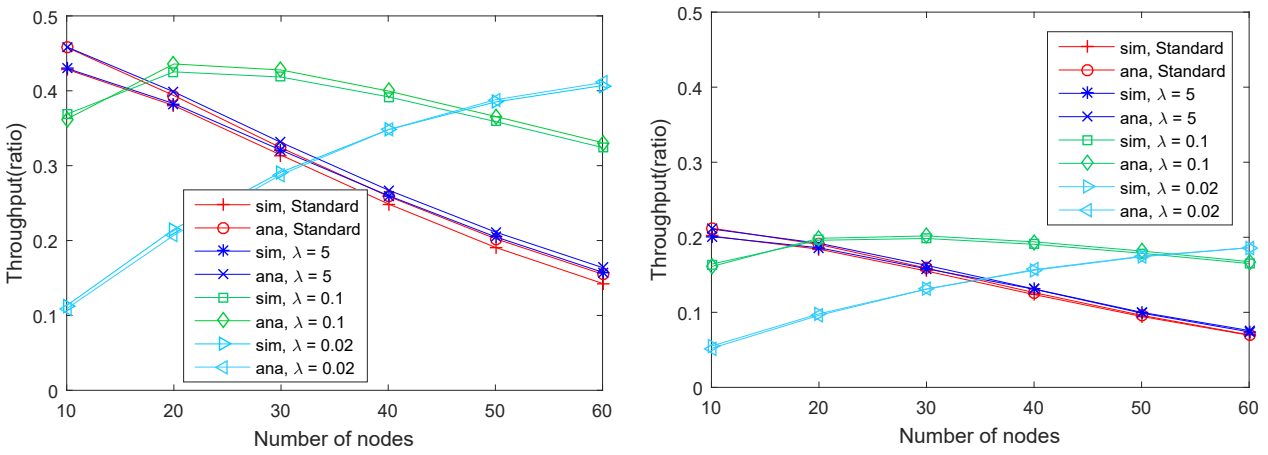


(a) $E_{\min} = 16$ for the network with energy limit, $L = 7$ backoff periods

(b) $E_{\min} = 11$ for the network with energy limit, $L = 2$ backoff periods

**Figure 3: The average throughput derived from the simulation (sim) and analytical model (ana) under different parameter setting. The parameter $E_{\max} = 30$ for the network with energy constraint, $q_0 = 0.3$, $m_0 = 3$ and $m = 4$**

energy unit per backoff period and this is used to tabulate the harvesting rate in the fourth column of Table 2. In the paper, we choose the harvesting rate $\lambda = 5, 0.1, 0.02$ as the simulation parameter, in which the rate = 5 is close to the rate given by outdoor solar energy harvesters, the rate = 0.1 is close to the rate given by electromagnetic energy harvesters, and rate = 0.02 is close to the rate given by thermoelectric energy harvesters.

Fig. 3 compares the average throughput derived from the simulation and our analytical model. The analytical model matches the simulation result closely. Subsequently, we analyze the throughput of the network under different energy harvesting rate $\lambda$. The energy harvesting rate is the average unit of the energy harvested in one backoff period. In our results, the curves/points labelled "standard" refer to the basic IEEE 802.15.4 protocol in which the devices have no energy constraint (i.e. no energy harvesting state in the model). It should be noted that the evaluation is also carried out under reasonable heavy traffic (i.e. $q_0 = 0.3$).

From the performance evaluation: (i) the throughput of the network with solar energy harvesting sources is almost equal to the throughput of network without energy constraint, and (ii) a higher energy harvesting rate yields a lower throughput. In line with our expectations, there is an upper bound on the throughput. Our evaluation also agrees with results from previous studies that show that energy harvesting directly affects the throughput, but our results go one step further and show that it is range bound (as evidenced by the asymptotic levelling of throughput). The reasoning behind the better performance is that energy harvesting nodes introduce lesser contention because of their intermittent transmission attempts which essentially reduces the overall attempts on the channel. It is well known that CSMA protocols suffer throughout degradation when large number of nodes compete for access [22], and in this case, the energy harvesting states reduces the number of devices contending for channel access thus improving throughput.

Next, we analyze the throughput of the network with different packet lengths $L$. By comparing Fig. 3(a) and Fig. 3(b), we observe that with the same number of nodes and the same energy harvesting rate, the network with longer packet length $L$ has better throughput. When $L$ becomes bigger, the value of $E_{\min}$ increases, which means that the number of times a device attempts to transmit a packet before the energy harvesting process starts may decrease. But the simulation result shows that the length of a packet $L$ has more influence than the value of $E_{\min}$ on the network throughput.

Figure 4 plots the average delay versus the number of nodes. The result of the analytical model tracks the simulation result well. We observe that the average delay of the network without the energy constraint is higher than the network with energy harvesting sources, and with the fixed number of nodes, the average delay decreases as the energy harvesting rate decreases. It is interesting that with lower energy harvesting rate, the delay increases faster as the number of nodes increases. By comparing Fig. 4(a) and Fig. 4(b), it is clear that with the same energy harvesting rate and the number of nodes, the larger packet lengths yields higher delay, and the delay is exaggerated when the number of nodes increase.

In Fig. 5, we seek to determine the network performance as a function of parameter $E_{\max}$. We compare the network throughput, delay and reliability with different energy harvesting rate and $E_{\max} = 30, 40, 50,$ and 60. We find that the performance difference is insignificant with increasing $E_{\max}$. Hence, we conclude that when the energy harvesting rate $\lambda$ is between 0.02 and 1 with $E_{\max}$ is between 30 to 60, $E_{\max}$ is not an important factor on the network performance.

Based on the results presented in Figs. 3–5, we demonstrated that our Markov chain model successfully predicts the behavior of the slotted CSMA/CA protocol of IEEE 802.15.4 standard with energy harvesting process. Additionally, we reaffirm previous findings [21] that the network performance is indeed different if the energy constraint of each device in considered.

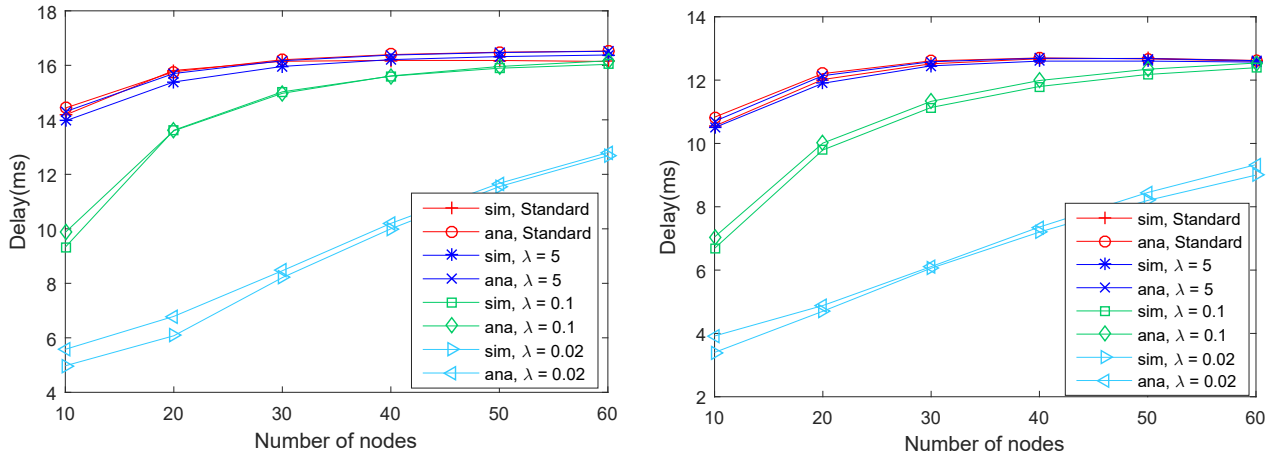


(a) $E_{\min} = 16$ for the network with energy limit, $L = 7$ backoff periods

(b) $E_{\min} = 11$ for the network with energy limit, $L = 2$ backoff periods

**Figure 4: The average delay derived from the simulation(sim) and analytical model(ana) under different parameter setting. The parameter $E_{\max} = 30$ for the network with energy constraint, $q_0 = 0.3$, $m_0 = 3$ and $m = 4$**

## 5. CONCLUSIONS

In this paper, we have analyzed the performance of the slotted CSMA/CA mechanism of the IEEE 802.15.4 standard taking into consideration the energy harvesting process in each IoT device. Insights to networked IoT performance with energy harvesting is expected to contribute to improving the prevailing energy constraints plaguing WSNs.

A Markov chain model is presented to analyze the performance of the slotted CSMA/CA mechanism with the energy harvesting process, and the performance is compared in terms of throughput, delay and reliability. The validity of the proposed model is proven by simulation. Analytical result shows that the performance of IoT devices with energy harvesting sources is different from typical CSMA/CA curves. We find that IoT devices with higher energy harvesting rate may have lower throughput if the network has large number of active nodes.

As the first attempt to incorporate energy harvesting process into the CSMA/CA mechanism for IEEE 802.15.4 standard, we make the assumption that the energy harvesting process follows the Poisson distribution and devices consume energy in discrete units. In practice, these assumptions may introduce errors into the predicted performance. Relaxing the above mentioned assumptions are immediate directions to improve the model and is left as the future work.

## 6. ACKNOWLEDGEMENT

This work was supported by Victoria University of Wellington's University Research Fund Grant #8-1620-207086-3468, by Excellent Research Projects of National Taiwan University under Grant 105R89082B, by Ministry of Science and Technology under Grant 105-2221-E-002-144-MY3, Information and Communications Research Laboratories of the Industrial Technology Research Institute (ICL/ITRI) and Institute for Information Industry (III).

## 7. REFERENCES

[1] *IEEE Std 802.15.4-2011, September, Part 15.4: Low-Rate Wireless Personal Area Networks (LR-WPANs)*. IEEE, 2011.

[2] E. Arias-Castro, J. Kleissl, and M. Lave. A Poisson model for anisotropic solar ramp rate correlations . *Solar Energy*, 101:192–202, 2014.

[3] Y. Chen, C.-A. Tan, M. Q. Feng, and Y. Fukuda. A video assisted approach for structural health monitoring of highway bridges under normal traffic. *Proc. SPIE*, 6174:1–18, 2006.

[4] N. Dang, R. Valentini, E. Bozorgzadeh, M. Levorato, and N. Venkatasubramanian. A Unified Stochastic Model for Energy Management in Solar-Powered Embedded Systems. In *Proc. of the IEEE/ACM International Conference on Computer-Aided Design (ICCAD)*, pages 621 – 626, 2015.

[5] Z. Eu, H. Tan, and W. Seah. Design and performance analysis of MAC schemes for Wireless Sensor Networks Powered by Ambient Energy Harvesting. *Ad Hoc Networks*, 9(3):300–323, 2011.

[6] D. M. Frangopol. Life-cycle performance, management, and optimisation of structural systems under uncertainty: accomplishments and challenges. *Structure and Infrastructure Engineering*, 7(6):389–413, 2011.

[7] J. Han, J. Hu, Y. Yang, Z. Wang, S. X. Wang, and J. He. A nonintrusive power supply design forself-powered sensor networks in the smartgrid by scavenging energy from ac power line. *IEEE Transactions on Industrial Electronics*, 62(7):4398–4407, 2015.

[8] C. K. Ho, P. D. Khoa, and P. C. Ming. Markovian Models for Harvested Energy in Wireless Communications. In *Proc. of IEEE International Conference on Communication Systems (ICCS)*, pages 311–315, 2010.

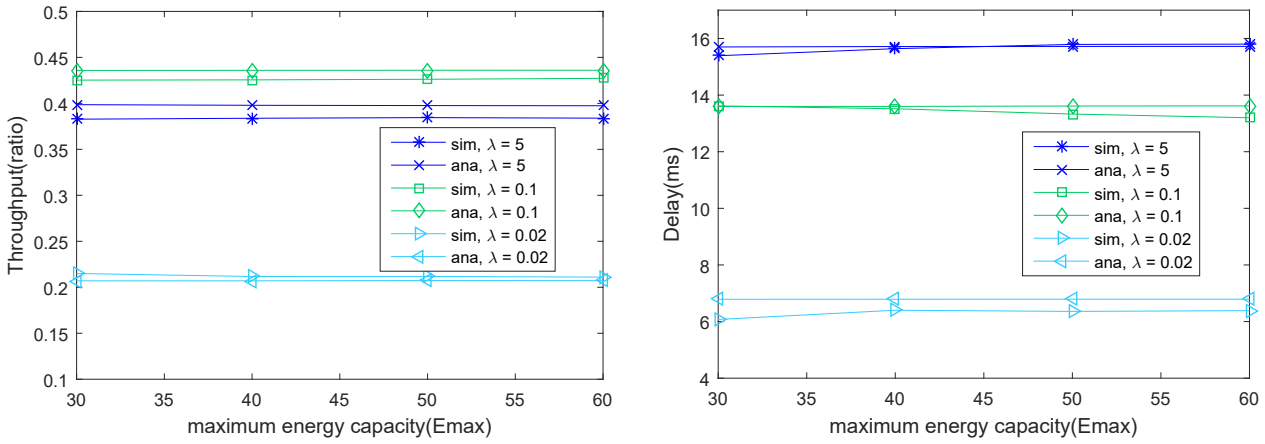


(a) Throughput

(b) Delay

**Figure 5: The average throughput and delay derived from the simulation(sim) and analytical model(ana) under different parameter setting. The parameter $N = 20$, $L = 7$ backoff periods, $q_0 = 0.3$, $m_0 = 3$ and $m = 4$**


[9] F. Iannello, O. Simeone, and U. Spagnolini. Medium Access Control Protocols for Wireless Sensor Networks with Energy Harvesting. *IEEE Transactions on Communications*, 60(5):1381 – 1389, 2012.

[10] A. Koubaa, M. Alves, and E. Tovar. A comprehensive simulation study of slotted CSMA/CA for IEEE 802.15.4 wireless sensor networks. In *Proc. of IEEE International Workshop on Factory Communication Systems*, pages 183–192, 28-30 June 2006.

[11] J. Lei, R. Yates, and L. Greenstein. A Generic Model for Optimizing Single-Hop Transmission Policy of Replenishable Sensors. *IEEE Transactions on Wireless Communications*, 8(2), 2009.

[12] V. Leonov. Thermoelectric energy harvesting of human bodyheat for wearable sensors. *IEEE Sensors Journal*, 13(6):2284–2291, 2013.

[13] J. Mišić, V. B. Mišić, and S. Shafi. Performance of a beacon enabled IEEE 802.15.4 cluster with downlink and uplink traffic. *IEEE Transactions on Parallel and Distributed Systems*, 17(4):361–376, 2006.

[14] NIWA. Solarview.

[15] P. Park, C. Fischione, and K. H. Johansson. Modeling and Stability Analysis of Hybrid Multiple Access in the IEEE 802.15.4 Protocol. *ACM Transactions on Sensor Networks*, 9(2), 2013.

[16] P. Park, P. D. Marco, P. Soldati, C. Fischione, and K. Johansson. A generalized Markov chain model for effective analysis of slotted IEEE 802.15.4. In *Proc. of IEEE 6th International Conference on Mobile Adhoc and Sensor Systems (MASS)*, pages 130–139, Macau, 12-15 Oct 2009.

[17] S. Pollin, M. Ergen, S. Ergen, B. Bougard, L. D. Perre, I. Moerman, A. Bahai, P. Varaiya, and F. Catthoor. Performance Analysis of Slotted Carrier Sense IEEE 802.15.4 Medium Access Layer. *IEEE Transactions on Wireless Communications*, 7(9):3359 – 3371, 2008.

[18] Post, E. Rehmi, and K. Waal. Electrostatic power harvesting for material computing. *Personal and Ubiquitous Computing*, 15(2):115–121, 2011.

[19] L. Ren, R. Chen, H. Xia, and X. Zhang. Energy harvesting performance of a broadband electromagnetic vibration energy harvester for powering industrial wireless sensor networks. *proc. SPIE*, 9799:1–11, 2016.

[20] W. K. G. Seah, Z. A. Eu, and H.-P. Tan. Wireless Sensor Networks Powered by Ambient Energy Harvesting (WSN-HEAP) - Survey and Challenges. In *Proc. of the 1st International Conference on Wireless*, pages 1–5, 2009.

[21] G. Yang, G.-Y. Lin, and H.-Y. Wei. Markov Chain Performance Model for IEEE 802.11 Devices with Energy Harvesting Source. In *Proc. of Global Communications Conference(GLOBECOM)*, pages 5212–5217, 2012.

[22] J. C. Yong, H. H. Young, S. D. Keun, and H. G. Uk. Enhanced Markov Chain Model and Throughput Analysis of the Slotted CSMACA for IEEE 802.15.4 Under Unsaturated Traffic Conditions. *IEEE Transactions on Vehicular Technology*, 58(1):473 – 478, 2009.

[23] A. Zanella, N. Bui, A. Castellani, and L. V. amd Michele Zorzi. Internet of things for smart cities. *IEEE Internet of Things Journal*, 1(1):22–32, 2014.